ANALYSIS OF THE AERODYNAMICS LOADS IN A CIRCULAR CYLINDER NEAR A MOVING GROUND

Alex Mendonça Bimbato, alexbimbato@unifei.edu.br
Luiz Antonio Alcântara Pereira, luizantp@unifei.edu.br
Universidade Federal de Itajubá, Instituto de Engenharia Mecânica, CP 50, Av. BPS 1303, Itajubá, MG, CEP. 37500-903

Miguel Hiroo Hirata, hirata@fat.uerj.br
FAT/UERJ, Campus Regional de Resende, Estrada Resende–Riachuelo, Resende, RJ

Abstract. *The mechanisms of the ground effect are still far from being fully understood due to a variety of other influencing factors, in particular the confusing influence of the boundary layer formed on the ground. The purpose of using the moving ground is to eliminate the influence of the boundary layer on the ground, which is probably one of the most crucial but confusing factors for this problem. In the present paper, we use a lagrangian mesh-free Vortex Method to calculate global as well a local quantities of high Reynolds number circular cylinder located near a moving ground flow. Vorticity only is generated from the circular cylinder surface and is discretized and represented by a cloud of Lamb discrete vortices. Each vortex in the cloud is accomplished in a purelly lagrangian description. The aerodynamics loads are computed using an integral formulation derived from the Poisson equation for the pressure. The numerical results for circular cylinder near a moving ground are compared with experimental results available in the literature.*

Keywords*: vortex method, moving ground, vortex shedding suppression, aerodynamics loads, bluff body*

1. INTRODUCTION

Viscous flow around circular cylinders has been studied by several authors during the last years not only to understand the fundamentals of general bluff body flows but also because this flow configuration itself is of direct relevance to many practical applications (e.g., tall buildings, bridge piers, chimneys, periscopes, heat exchangers tubes, cables, wires, and so on).

In fact, the flow around cylinders includes a variety of fluid dynamics phenomena, such as separation, vortex-shedding and the transition to turbulence.

The well-known Karman-type vortex shedding may occur behind the cylinder, the control or suppression of which is of great interest in many engineering applications. It is reasonable to focus on flow around bodies of simple geometry to understand such general complex flows systematically. Bluff bodies (one particular example is the flow around circular cylinders) having a two-dimensional structure are very suitable for restricting the complexity and thus observing the fundamentals features of the flow.

The problem with a circular cylinder close to a plane wall is governed not only by the Reynolds number but also by ratio of the gap between the cylinder and the ground, i.e., the gap ratio defined by h/d (d is diameter of cylinder). The fundamental effects of gap ratio have been successfully observed by Taneda (1965), Roshko *et al.* (1975), Bearman and Zdravkovich (1978), Burest and Lanciotti (1979), Angrilli *et al.* (1982), Grass *et al.* (1984), Zdravkovich (1985a), Price *et al.* (2002) and Lin *et al.* (2005).

However, the influence of the boundary layer formed on the ground is much more complicated and is still unclear despite several intensive studies reported so far. Roshko *et al.* (1975) measured the time-averaged drag and lift coefficients, C_D and C_L, for a circular cylinder placed near a fixed wall in a wind tunnel at $Re=2.0\times10^4$, which lies in the upper-subcritical flow regime, and showed that the C_D rapidly decreased and C_L increased as the cylinder came close to the wall. Zdravkovich (1985b) observed, in his force measurements performed at $4.8\times10^4 < Re < 3.0\times10^5$, that the rapid decrease in drag occurred as the gap was reduced to less than the tickness of the boundary layer δ/d on the ground, and concluded that the variation of C_D was dominated by h/δ rather than by the conventional gap ratio h/d. He also noted that the C_L could be significantly affected by the state of the boundary layer, although it was insensitive to the tickness of the boundary layer.

Zdravkovich (2003) reported the drag behavior for cylinder placed near a moving ground running at the same speed as the freestream for higher Reynolds number of 2.5×10^5, which lies within the critical flow regime rather than the subcritical flow regime. The experiment by Zdravkovich (2003) showed contrast to all the above studies. First, practically no boundary layer on the ground. Second, the decrease in drag due the decrease in h/d did not occur in his measurements. The differences encountered were attributed to the non-existence of the wall boundary layer or the higher Reynolds number, or any other influencing factors.

Nishino *et al.* (2007) presented experimental results of a circular cylinder with an aspect ratio of 8.33, with and without end-plates, placed near and parallel to a moving ground, on which substantially no boundary layer developed to interface with the cylinder. The main purpose of experiments was to elucidate the fundamental mechanisms of ground

effect in more details by using a moving ground running at the same speed as the freestream and thereby eliminating the confusing effects of boundary layer formed on the ground. Measurements were carried out at two upper-subcritical Reynolds numbers of 0.4 and 1.0×10^5. The results produced new insights into the physics of ground effect, and could serve as a database for both experimental and computational studies on the ground effect in the future. According to Nishino *et al.* (2007) experiments, for the cylinder with end-plates, on which the oil flow patterns were observed to be essentially two-dimensional, the drag rapidly decrease as h/d decrease to less than 1.0 but became constant for h/d of less than 0.85, unlike that usually observed near a fixed ground (as will be plotted later in "Fig. 2a").

In the present paper, the Vortex Method is employed to simulate numerically the vortex-shedding flow from a circular cylinder near a moving ground. The two-dimensional aerodynamics characteristics are investigated at a Reynolds number of 1.0×10^5 and comparisons are made with experimental results presented by Nishino *et al.* (2007). The main purpose of present numerical study is the investigation of the ground effect in more details by using a moving ground running at the same speed as the freestream and thereby eliminating the confusing effects of the boundary layer formed on the ground.

The Vortex Method have been developed and applied for analysis of complex, unsteady and vortical flows in relation to problems in a wide range of industries, because they consist of simple algorithm based on physics of flow (Kamemoto, 2004). Vortex cloud modeling offers great potential for numerical analysis of important problems in fluid mechanics. A cloud of free vortices is used in order to simulate the vorticity, which is generated on the body surface and develops into the boundary layer and the viscous wake. Each individual free vortex of the cloud is followed during the numerical simulation in a typical Lagrangian scheme. This is in essence the foundations of the Vortex Method (Chorin, 1973; Sarpakaya, 1989; Lewis, 1999; Kamemoto, 2004; Alcântara Pereira *et al.*, 2004; Stock 2007).

Vortex Method offers a number of advantages over the more traditional Eulerian schemes: (a) the absence of a mesh avoids stability problems of explicit schemes and mesh refinement problems in regions of high rates of strain; (b) the Lagrangian description eliminates the need to explicitly treat convective derivatives; (c) all the calculation is restricted to the rotational flow regions and no explicit choice of the outer boundaries is needed a priori; (d) no boundary condition is required at the downstream end of the flow domain.

For the grid methods, such as finite difference method and finite element method, the governing Navier-Stokes equations are solved directly. However, the flows around cylinders are usually computed at Reynolds number up to a few hundred while the Re for flows around cylinders in many engineering applications is of much higher order O (10^6). In such circumstance, the traditional Eulerian schemes will not give a satisfactory prediction within a reasonable computational cost. Also, the pre-processing and mesh-generation are time-consuming for the grid method in numerical simulations.

The authors of this paper has developed the present Vortex Method to simulate the macro scale phenomena, therefore the smaller scale ones are taken into account through the use of a second order velocity function (Alcântara Pereira et *al*., 2002). In the present paper, the effects of small scale are not still considered.

2. GOVERNING EQUATIONS

Consider the incompressible flow of a Newtonian fluid around a circular cylinder in an unbounded two-dimensional region near a moving ground. "Figure 1" shows the incident flow, defined by free stream speed U and the domain Ω with boundary $S = S_1 \cup S_2 \cup S_3$, S_1 being the body surface, S_2 being the ground surface running at the same speed as the incident flow and S_3 the far away boundary.

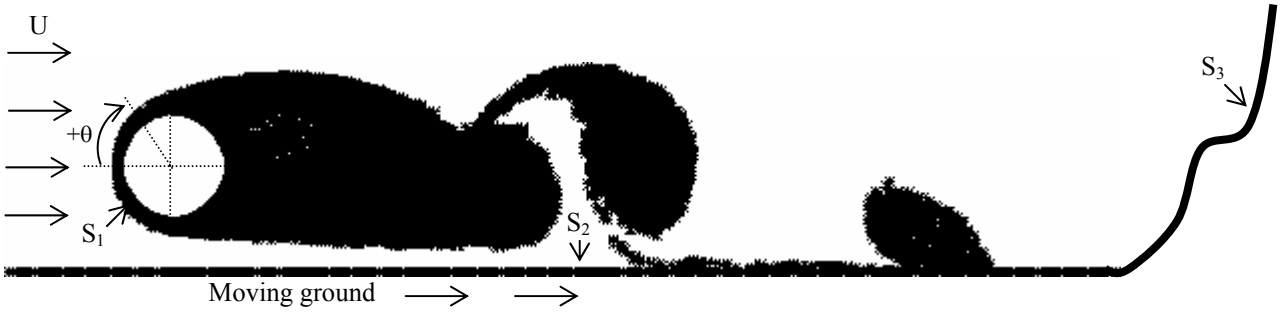

Figure 1. Circular cylinder near a moving ground

The viscous and incompressible flow is governed by the continuity and the Navier-Stokes equations, which can be written in the form

$$\nabla \cdot \mathbf{u} = 0 \tag{1}$$

$$\frac{\partial \mathbf{u}}{\partial t} + \mathbf{u} \cdot \nabla \mathbf{u} = -\nabla p + \frac{1}{Re} \nabla^2 \mathbf{u} . \tag{2}$$

In the equations above $\mathbf{u}$ is the velocity vector field and p is the pressure. As can be seen the equations are non-dimensionalized in terms of U and d (diameter cylinder). The Reynolds number is defined by

$$Re = \frac{dU}{\upsilon} \tag{2a}$$

where υ is the fluid kinematics viscosity coefficient; the dimensionless time is d/U.

The impermeability and no-slip conditions on the body surface and the only impermeability condition on the moving ground are written as

$$u_n = \mathbf{u} \cdot \mathbf{e}_n = 0 \tag{3a}$$

$$u_\tau = \mathbf{u} \cdot \mathbf{e}_\tau = 0 \tag{3b}$$

$\mathbf{e}_n$ and $\mathbf{e}_\tau$ being, respectively, the unit normal and tangential vectors. One assumes that, far away, the perturbation caused by the body and moving ground fades as

$$|\mathbf{u}| \to 1 \text{ at } S_3 . \tag{3c}$$

The dynamics of the fluid motion, governed by the boundary-value problem (1), (2) and (3), can be alternatively studied by taking the curl of "Eq. (2)", obtaining the well-known 2-D vorticity transport equation

$$\frac{\partial \omega}{\partial t} + \mathbf{u} \cdot \nabla \omega = \frac{1}{Re} \nabla^2 \omega \tag{4}$$

in which ω is the only non-zero component of the vorticity vector.

3. SOLUTION METHOD

The solution method applied in this paper has been developed by Alcântara Pereira *et al.* at the Federal University of Itajubá. According to the convection-diffusion splitting algorithm (Chorin, 1973) it is assumed that in the same time increment the convection and the diffusion of the vorticity can be independently handled and are governed by

$$\frac{\partial \omega}{\partial t} + \mathbf{u} \cdot \nabla \omega = 0 \tag{5}$$

$$\frac{\partial \omega}{\partial t} = \frac{1}{Re} \nabla^2 \omega . \tag{6}$$

Convection is governed by "Eq. (5)" and the velocity field is given by

$$\mathbf{u}(\mathbf{x}, t) = \mathbf{ui}(\mathbf{x}, t) + \mathbf{ub}(\mathbf{x}, t) + \mathbf{uv}(\mathbf{x}, t) . \tag{7}$$

The contribution of the incident flow is represented by **ui** (**x**, t). For an uniform oncoming flow its components take the form

$$ui_1 = 1 \text{ and } ui_2 = 0 . \tag{8}$$

The body and moving ground contribute with **ub**(**x**,t), which can be obtained, for example, using the Boundary Element Method. The two components can be written as

$$ub_i(\xi,t) = \sum_{j=1}^{M} \sigma_j G_{ij}(\xi - \xi_j(t)),\ i = 1, 2, \tag{9}$$

where $G_{ij}(\xi - \xi_j(t))$ is an appropriated defined kernel (Katz and Plotkin, 1991). In this paper sources with constant density, σ_j, were distributed over M flat panels representing the body surface and the moving ground plane.

Finally the velocity **uv**(**x**, t), due to the vortex-vortex interaction (Biot-Savart´s Law) has its components written as

$$uv_i(x,t) = \sum_{j=1}^{Z} \Gamma_j c_{ij}(x - x_j(t)),\ i = 1, 2. \tag{10}$$

Here, Γ_j is the j-vortex strength and $c_{ij}(\mathbf{x} - \mathbf{x}_j(t))$ is the i component of the velocity induced, at point **x**, by a unit strength vortex located at x_j (t). We use Lamb vortex, therefore

$$u_\theta^{kj} = -\frac{\Gamma_j}{2\pi}\frac{1}{r_{kj}}\left[1 - \exp\left(-5{,}02572\frac{r_{kj}^2}{\sigma_0^2}\right)\right] \tag{10a}$$

where σ_0 is core radius of the Lamb vortex (Mustto *et al.*, 1998).

The process of vorticity generation from the circular cylinder surface is carried out from "Eq. (3b)", so as to satisfy the no-slip condition. According to the discussion above the panels method guaranties that the impermeability condition is satisfied in each straight-line element, or panel, at pivotal point. At each instant of the time MB new vortices are created at a small distance ε of the body surface, whose strengths are determined from "Eq. (3b)" applied at MB point's right below the newly created vortices, along the radial direction. This procedure yields an algebraic system of MB equations and MB unknowns (the strengths of the vortices).

Each vortex particle distributed in the flow field is followed during numerical simulation according to the first order Euler scheme

$$z_k(t + \Delta t) = z_k(t) + u_k(t)\Delta t + \xi_k, \tag{11}$$

in which z_k is the position of a particle, Δt is the time increment and ξ_k is the random walk displacement. According to Lewis (1999), the random walk displacement is given by

$$\xi_k = \sqrt{4\beta\Delta t \ln\left(\frac{1}{P}\right)}\left[\cos(2\pi Q) + i\sin(2\pi Q)\right] \tag{12}$$

where $\beta = Re^{-1}$, $i = \sqrt{-1}$, P and Q are random numbers between 0.0 and 1.0.

The pressure calculation starts with the Bernoulli function, defined by Uhlman (1992) as

$$Y = p + \frac{u^2}{2},\ u = |\mathbf{u}|. \tag{13}$$

Kamemoto (1993) used the same function and starting from the Navier-Stokes equations was able to write a Poisson equation for the pressure. This equation was solved using a finite difference scheme. Here the same Poisson equation was derived and its solution was obtained through the following integral formulation (Shintani and Akamatsu, 1994)

$$H\overline{Y_i} - \int_{S_1} \overline{Y}\nabla G_i \cdot \mathbf{e}_n dS = \iint_\Omega \nabla G_i \cdot (\mathbf{u}\times\boldsymbol{\omega}) d\Omega - \frac{1}{Re}\int_{S_1} (\nabla G_i \times \boldsymbol{\omega}) \cdot \mathbf{e}_n dS \tag{14}$$

where H is 1.0 inside the flow (at domain Ω) and is 0.5 on the boundaries S_1 and S_2. $G_i = (1/2\pi)\log R^{-1}$ is the fundamental solution of Laplace equation, R being the distance from ith vortex element to the field point.

It is worth to observe that this formulation is specially suited for a Lagrangian scheme because it utilizes the velocity and vorticity field defined at the position of the vortices in the cloud. Therefore it does not require any

additional calculation at mesh points. Numerically, "Eq. (14)" is solved by mean of a set of simultaneous equations for pressure Y_i.

4. RESULTS AND DISCUSSIONS

Before discussing the results for circular cylinder in moving ground, we present the results for cylinder not placed near a boundary or ground. The cylinder surface was represented by MB=300 flat source panels with constant density. The simulation was performed up to 1000 time steps with magnitude Δt=0.05. During each time step the new vortex elements are shedding into the cloud through a displacement $\varepsilon=\sigma_0$=0.001d normal to the straight-line elements (panels). The aerodynamics loads computations are computed between t=28.3 and t=48.0, "Fig. 3a". The results of the numerical simulation are presented in "Tab. 1". In this table one can find also experimental (Blevins (1984) with 10% uncertainty) and numerical (Mustto *et al.* (1998)) results. The observation to note here is that the mean numerical lift coefficient is not zero due to the numerical errors.

Table 1. Comparisons of the mean drag coefficient and Strouhal number with other numerical and experimental results for a circular cylinder without ground effect

$Re = 10^5$	$\overline{C_D}$	$\overline{C_L}$	$\overline{St}$
Blevins (1984)	1.20	-	0.19
Mustto *et al.* (1998)	1.22	-	0.22
Present Simulation	1.25	0.02	0.21

The numerical results of Mustto *et al.* (1998) were also obtained using the Vortex Method associated to the Circle Theorem (Milne-Thompson, 1955) while the panels method was used in the present simulation. The agreement between the two numerical methods is very good for the Strouhal number, and both results are close to the experimental value. The present drag coefficient shows a higher value as compared to the experimental result. One should observe, that the three-dimensional effects are non-negligible for the Reynolds number used in the present simulation ($Re=1.0\times10^5$). Therefore one can expect that a two-dimensional computation of such a flow must produce higher values for the drag coefficient. On the other hand, the Strouhal number is insensitive to these three-dimensional effects. Computed values for time-averaged drag and lift coefficients for circular cylinder in moving ground are plotted in "Fig. 2".

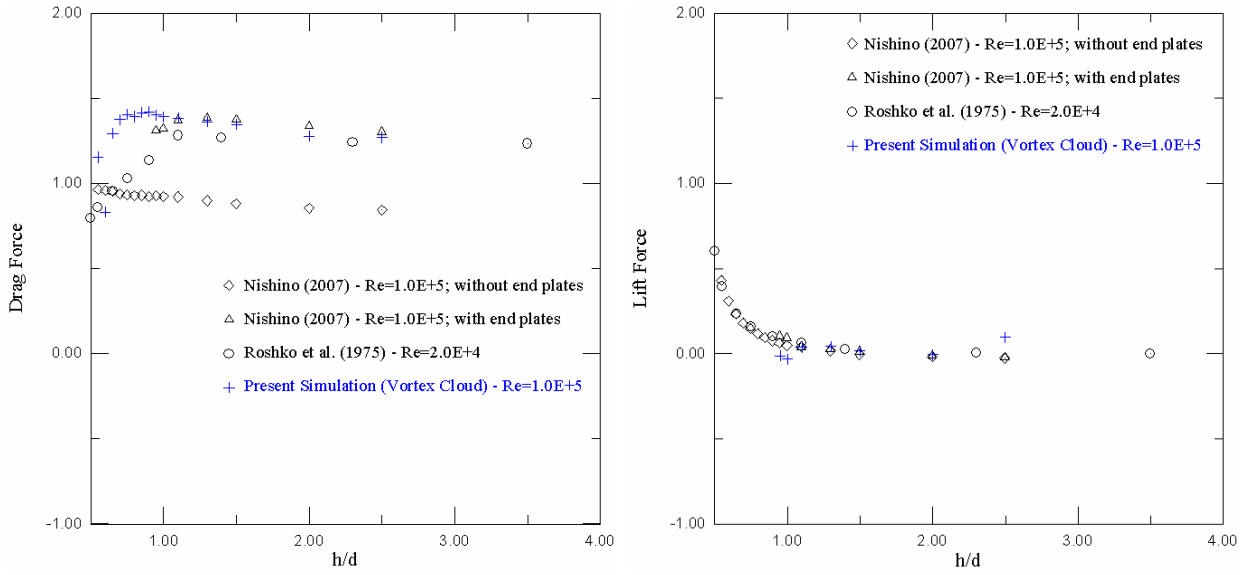

(a) Drag force (b) Lift force

Figure 2. Time-averaged drag and lift coefficients *vs.* gap ratio for different end conditions

As expected the simulation results follow the end plates curve. The drag behaviour, see "Fig. 2a", observed for the cylinder with end plates was totally different from that for the cylinder without end plates. For the cylinder with end plates the flow characteristics are essentially two-dimensional, the drag rapidly decrease as h/d decrease to less than 1.00. The critical drag behavior was found to be directly related to a global change in the near wake structure of the

cylinder. For the cylinder without end plates, however, no such critical change in drag was observed as the Karman-type vortices were not generated in the wake region at all h/d investigated by Nishino *et al.* (2007). The results for a fixed ground by Roshko *et al.* (1975) are also showed here for the purpose of comparison. "Figure 3" shows that the time-averaged lift coefficient behaviour observed in this study is similar to that reported by Roshko *et al.* (1975), see "Fig. 2b".

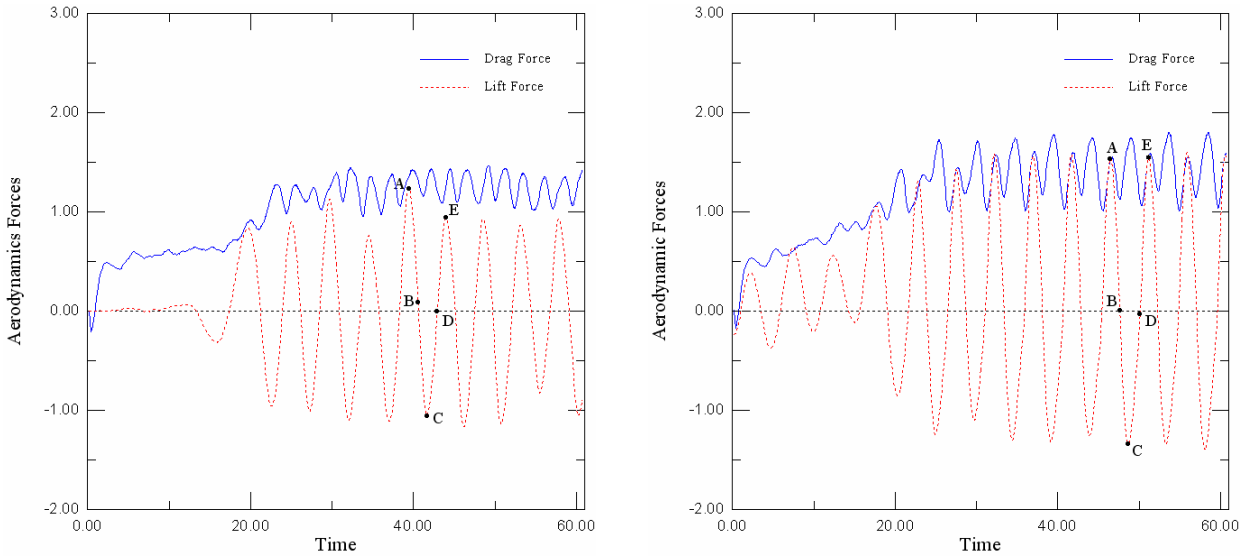

(a) Computed without moving ground (h/d=1000) (b) Computed with moving ground (h/d=0.95)

Figure 3. Time history of the aerodynamics at Reynolds number Re=1.0×10^5

"Figure 4" shows plots of instantaneous pressure distributions around circular cylinder surface with and without moving ground. Point B of the "Fig. 4b" is defined by an instant in which the C_D curve presents a minimum value (see "Fig. 3b"), point C by an adjacent maximum and point D by a minimum again. At the instant represented by the point A one can clearly observe low pressure distribution on the rear part of the cylinder when the drag curve assumes maximum value (in our computations the tangential stress was not considered).

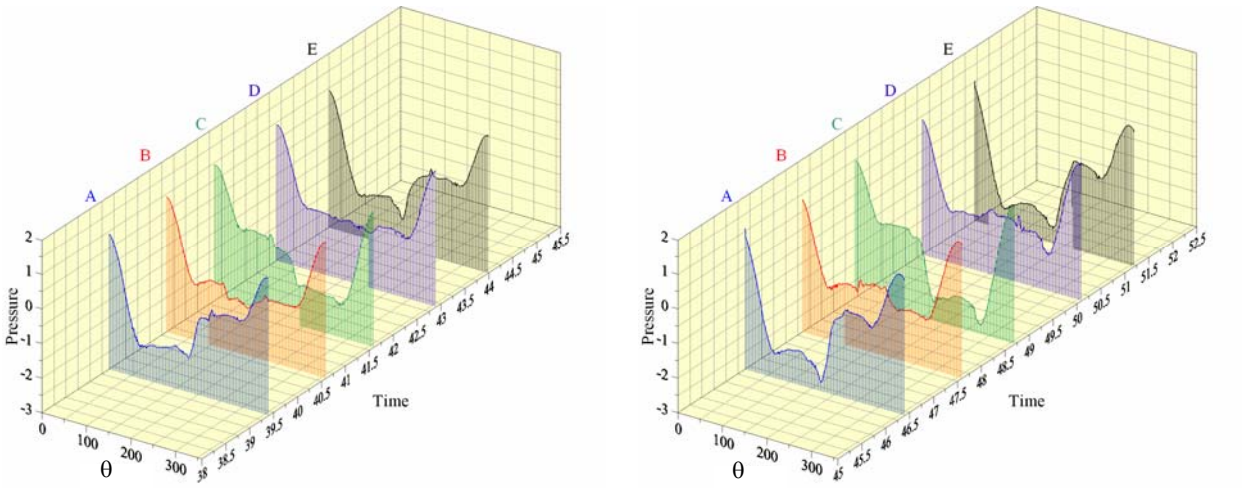

(a) Computed without moving ground (h/d=1000) (b) Computed with moving ground (h/d=0.95)

Figure 4. Predicted pressure distribution on a circular cylinder at Reynolds number Re=1.0×10^5

The near field flow pattern shows that at instant A one can observe an already started clockwise vortex structure at the upper side of the cylinder (see "Fig. 5a"). This structure as well as the drag coefficient increases with time (see "Fig. 3a"). At this very moment the vortex structure detaches from the rear part of the cylinder surface and is incorporated to the viscous wake at the instant B; this process creates a low pressure region at the rear part of the cylinder which is associated to the high drag value, see "Fig. 4a". Right after the process a new anti-clockwise vortex structure starts at the low side of the cylinder surface and the above described sequence of events repeats all over again.

Figure 6 shows near field flow pattern at instant A and instant B when a cylinder is located near a moving ground by the gap ratio h/d=0.95. Here, the above describe sequence of events repeats all over again. Note in the "Fig. 3b" that when the C_D curve presents a maximum value, the C_L curve presents maximum value (point A) or minimum value (point C). Compare this forces behavior with that showed in "Fig. 3a".

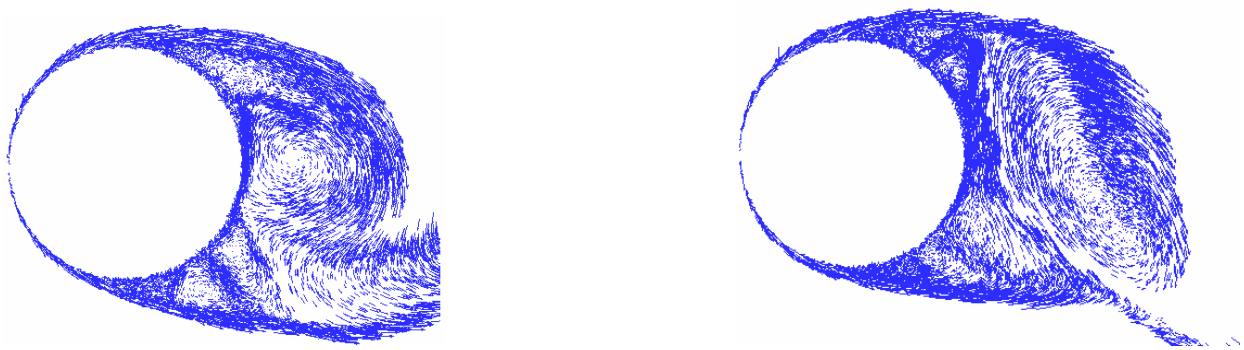

(a) Point A (b) Point B

Figure 5. Near field velocity distribution without moving ground (h/d=1000)

The ground surface was represented by MG=300 source panels with constant density. Each simulation required 133 h of CPU time in an Intel(R) Pentium (R) 4 CPU 1700 MHz. Our method, therefore, is able to provide good estimates for drag coefficient, and able to predict the flow correctly in a physical sense.

(a) Point A (b) Point B

Figure 6. Near field velocity distribution with moving ground (h/d=0.95).

5. CONCLUSIONS

The main objective of the work was to implement the algorithm and to get some insight into the potentialities of the model developed; this was accomplished since the results show that the behavior of the quantities of interest is the expected one. Some discrepancies observed in the determination of the aerodynamics loads may be attributed to errors in the treatment of vortex element moving away from a solid surface. Because every vortex element has different strength of vorticity, it will diffuse to different location in the flow field. It seems impossible that every vortex element will move to same ε-layer normal to the solid surface (Yang and Huang, 1999). In the present method all nascent vortices were placed into the cloud through a displacement $\varepsilon=\sigma_0=0.001d$ normal to the panels. The sub-grid turbulence modeling is of significant importance for the present numerical simulation. The development of Lagrangian LES models for Vortex Method has been discussed in the literature. In the present study, a methodology for the numerical simulation of a viscous turbulent flow will be carried out (Alcântara Pereira *et al.*, 2002). From the present study, is confirmed that the methodology used here is convenient for investigation of unsteady characteristics of the flow.

6. ACKNOWLEDGEMENTS

The authors would like to acknowledge FAPEMIG (Proc. TEC-748/04) and CNPq for the financial support during the time of this project.

7. REFERENCES

Alcântara Pereira, L.A., Hirata, M.H. and Manzanares Filho, N. 2004, "Wake and Aerodynamics Loads in Multiple Bodies - Application to Turbomachinery Blade Rows", J. Wind Eng. Ind Aerodyn., 92, pp. 477-491.
Alcântara Pereira, L.A., Ricci, J.E.R., Hirata, M.H. and Silveira-Neto, A., 2002, "Simulation of Vortex-Shedding Flow about a Circular Cylinder with Turbulence Modeling", Intern'l Society of CFD, Vol. 11, No. 3, October, pp. 315-322.
Angrilli, F, Bergamaschi, S. and Cossalter, V., 1982, "Investigation of Wall Induced Modifications to Vortex Shedding from a Circular Cylinder", Transactions of the ASME: Journal of Fluids Engineering, Vol. 104, pp. 518-522.
Bearman, P.W. and Zdravkovich, M.M., 1978, "Flow around a Circular Cylinder near a Plane Boundary", Journal of Fluid Mechanics, Vol. 89, pp. 33-47.
Blevins, R.D., 1984, "Applied fluid dynamics hanbook", Van Nostrand Reinhold Co.
Buresti, G. and Lanciotti, A., 1979, "Vortex Shedding from Smooth and Roghened Cylinders in Cross-Flow near a Plane Surface", Aeronautical Quarterly, Vol. 30, pp. 305-321.
Chorin, A.J., 1973, "Numerical Study of Slightly Viscous Flow", Journal of Fluid Mechanics, Vol. 57, pp. 785-796.
Grass, A.J., Raven, P.W.J., Stuart, R.J. and Bray, J.A., 1984, "Influence of Boundary Layer Velocity Gradientes and Bed Proximity on Vortex Shedding from Free Spanning Pipelines", Transactions of the ASME: Journal of Energy Resources Technology, Vol. 106, pp. 70-78.
Kamemoto, K., 2004, "On Contribution of Advanced Vortex Element Methods Toward Virtual Reality of Unsteady Vortical Flows in the New Generation of CFD", Proceedings of the 10th Brazilian Congress of Thermal Sciences and Engineering-ENCIT 2004, Rio de Janeiro, Brazil, Nov. 29 - Dec. 03, Invited Lecture-CIT04-IL04.
Kamemoto, K., 1993, "Procedure to Estimate Unstead Pressure Distribution for Vortex Method" (In Japanese), Trans. Jpn. Soc. Mech. Eng., Vol. 59, No. 568 B, pp. 3708-3713.
Katz, J. and Plotkin, A., 1991, "Low Speed Aerodynamics: From Wing Theory to Panel Methods". McGraw Hill, Inc.
Lewis, R.I., 1999, "Vortex Element Methods, the Most Natural Approach to Flow Simulation - A Review of Methodology with Applications", Proceedings of 1st Int. Conference on Vortex Methods, Kobe, Nov. 4-5, pp. 1-15.
Lin, C., Lin, W.J. and Lin, S.S., 2005, "Flow Characteristics around a Circular Cylinder near a Plane Boundary", Proceedings of the Sixteenth International Symposium on Transport Phenomena (ISTP-16), 29 August – 1 September, Prague, Czech Republic, (CD-ROOM).
Milne-Thompson, L.M., 1955, "Theoretical and Hydrodynamics", MacMillan & Co.
Mustto, A.A., Hirata, M.H. and Bodstein, G.C.R., 1998, "Discrete Vortex Method Simulation of the Flow Around a Circular Cylinder with and without Rotation", A.I.A.A. Paper 98-2409, Proceedings of the 16th A.I.A.A. Applied Aerodynamics Conference, Albuquerque, NM, USA, June.
Nishino, T., Roberts, G.T. and Zhang, X., 2007, "Vortex Shedding from a Circular Cylinder near a Moving Ground", Physics of Fluids, Vol. 19, 025103.
Price, S.J., Summer, D., Smith, J.G., Leong, K. and Paidoussis, M.P., 2002, "Flow Vizualization around a Circular Cylinder near to a Plane Wall", Journal of Fluids ans Structures, Vol. 16, pp. 175-191.
Roshko, A., Steinolfson, A. and Chattoorgoon, V., 1975, "Flow Forces on a Cylinder near a Wall or near Another Cylinder", Proceedings of the 2nd US Nation Conference on Wind Engineering Research, Fort Collins, Paper IV-15.
Sarpkaya, T., 1989, "Computational Methods with Vortices - The 1988 Freeman Scholar Lecture", Journal of Fluids Engineering, Vol. 111, pp. 5-52.
Shintani, M. and Akamatsu, T, 1994, "Investigation of Two Dimensional Discrete Vortex Method with Viscous Diffusion Model", Computational Fluid Dynamics Journal, Vol. 3, No. 2, pp. 237-254.
Stock, M.J., 2007, "Summary of Vortex Methods Literature (A lifting document rife with opnion)", April 18, 2007.
Taneda, S., 1965, "Experimental Investigation of Vortex Streets", Journal of the Physical Society of Japan, Vol. 20, pp. 1714-1721.
Uhlman, J.S., 1992, "An Integral Equation Formulation of the Equation of an Incompressible Fluid", Naval Undersea Warfare Center, T.R. 10-086.
Yang, R.J. and Huang, Y.G., 1999, "Simulation of High Reynolds Flow Over a Flat Plate by a Deterministic Vortex Method", Comput. Fluid Dynamics Journal, Vol. 8, No. 2.
Zdravkovich, M.M., 1985a, "Observation of Vortex Shedding behind a Towed near a Wall", Flow Visualization III: Proceedings of the Third International Symposium on Flow Vizualization, ed. W.J. Yang, Hemisphere, Washington DC, pp. 423-427.
Zdravkovich, M.M., 1985b, "Forces on a Circular Cylinder near a Plane Wall", Applied Ocean Research, Vol. 7, pp. 197-201.
Zdravkovich, M.M., 2003, "Flow around Circular Cylinders" Vol. 2: Applications, Oxford University Press, Oxford, UK.

8. RESPONSIBILITY NOTICE

The authors are the only responsible for the printed material included in this paper.